GaSb/GaP compliant interface for high electron mobility AlSb/InAs heterostructures on (001) GaP

S. El Kazzi, L. Desplanque, Christophe Coinon, Y. Wang, P. Ruterana, X. Wallart

GaSb/GaP compliant interface for high electron mobility AlSb/InAs heterostructures on (001) GaP

Cite as: Appl. Phys. Lett. **97**, 192111 (2010); https://doi.org/10.1063/1.3515867
Submitted: 28 September 2010 • Accepted: 20 October 2010 • Published Online: 12 November 2010

S. El Kazzi, L. Desplanque, C. Coinon, et al.

GaSb/GaP compliant interface for high electron mobility AlSb/InAs heterostructures on (001) GaP

S. El Kazzi,[1] L. Desplanque,[1,a)] C. Coinon,[1] Y. Wang,[2] P. Ruterana,[2] and X. Wallart[1]
[1]*Institut d'Electronique, de Microélectronique, et de Nanotechnologie, UMR-CNRS 8520, BP 60069, 59652 Villeneuve d'Ascq Cedex, France*
[2]*CIMAP UMR 6252 CNRS-ENSICAEN-CEA-UCBN, 6, Boulevard du Maréchal Juin, 14050 Caen Cedex, France*

(Received 28 September 2010; accepted 20 October 2010; published online 12 November 2010)

We report on the epitaxial growth of an AlSb/InAs heterostructure on a (001) GaP substrate. We investigate the conditions for the most efficient relaxation of GaSb islands on GaP. In particular, we show that the GaP surface treatment and the growth temperature are crucial for the formation of a two-dimensional periodic array of 90° misfit dislocations at the episubstrate interface. With this relaxation process, an AlSb/InAs heterostructure exhibiting a room temperature mobility of 25 500 $cm^2 V^{-1} s^{-1}$ on GaP is demonstrated. This result paves the way to the integration of Sb-based devices on Si substrates through the use of GaP/Si templates. © *2010 American Institute of Physics*. [doi:10.1063/1.3515867]

Although Sb-based devices have demonstrated promising performances in high frequency electronics,[1] their development toward large scale applications has been greatly impeded by the lack of large-size, low-cost, lattice-matched, and commercially available substrates. Since the pioneering work of Chang *et al.*,[2] AlSb/InAs heterostructures exhibiting electron mobility higher than 30 000 $cm^2 V^{-1} s^{-1}$ have been demonstrated on GaAs or InP substrates using a GaSb or an AlSb metamorphic buffer layer.[1,3,4] Moreover, it has been shown that the initial growth of GaSb or AlSb leads to the formation of relaxed islands by periodic 90° misfit dislocations (MDs) corresponding to the three-dimensional (3D) Volmer–Weber growth mode.[5–9]

Besides the mismatch problem, if no particular attention is taken [for instance, atomic layer molecular beam epitaxy in the case of GaAs/Si (Ref. 10)], the direct growth of antimonides on silicon involves, like for other polar III-V materials, the formation of antiphase domains (APDs). Some attempts using an AlSb nucleation layer have been reported,[11,12] demonstrating very low threading defect densities and APDs when a 5° miscut (001) Si substrate is used.[13] However, exactly oriented Si substrates are the standard ones in the current Si technology. Recently, APD-free GaP layers on exactly oriented (001) Si substrates have been achieved after 50 nm overgrowth.[14] These templates could be used for the subsequent growth of antimonides.

For this reason, we investigate in this paper the initial steps of the growth of GaSb on GaP. More precisely, we study the influence of the surface preparation and growth temperature on the relaxation of GaSb islands on GaP. Under optimized conditions, we demonstrate an AlSb/InAs heterostructure with a room temperature (RT) mobility exceeding 25 000 $cm^2 V^{-1} s^{-1}$.

The samples are grown by molecular beam epitaxy on exactly oriented (001) $\pm 0.1°$ GaP substrates in a Riber 32P chamber equipped with groups III and V sources and silicon for n-type doping. The phosphorous flux is obtained by cracking phosphine (PH_3) through a high-temperature injector, whereas a valve-cracker cell is used to produce Sb_2. Group III elements and Sb fluxes are calibrated via reflection high energy electron diffraction (RHEED) specular beam intensity oscillations on GaAs, InAs, and GaSb. A V/III ratio between two and three and typical growth rates between 0.7 and 1 ML/s are used during the growth. After the deoxidization of the GaP substrates at 650 °C, a 400 nm GaP buffer layer is grown at 610 °C to obtain a smooth GaP surface exhibiting a sharp (2×4) RHEED pattern. After the homoepitaxy, the phosphine flux is interrupted.

Two samples (A and B) are first grown to study the influence of the GaP surface treatment on the relaxation of 10 GaSb ML. For sample A, the substrate is cooled down from 610 to 480 °C without any flux, keeping a (2×4) surface reconstruction, and then 1 Ga ML is deposited before the opening of the Sb valve with a subsequent growth of 9 GaSb ML without any interruption. For sample B, after the interruption of the phosphine flux, the substrate is cooled down to 480 °C under Sb_2. The RHEED pattern exhibits an incomplete $\times6$ reconstruction in the $[1\bar{1}0]$ azimuth, whereas a $\times8$ reconstruction is observed in the [110] one. Then the Ga shutter is opened and 10 GaSb ML are deposited. A second set of samples (C, D, and E) is grown to investigate the role of the growth temperature between 450 and 530 °C with the same epitaxial sequence as sample B. The surface morphology of the samples is examined by atomic force microscopy (AFM) using a Digital Nanoscope III system, working in the tapping mode. The structural properties are investigated by transmission electron microscopy (TEM) using a JEOL 2010 FEG instrument operated at 200 kV.

For both samples A and B, once the GaSb growth begins, the RHEED pattern turns rapidly from a two-dimensional to a 3D one, characteristic of a Volmer–Weber growth mode. After a few monolayers, a (1×3) surface reconstruction, characteristic of the (001) GaSb surface, starts to appear. Strain relaxation of GaSb is investigated using the RHEED pattern analysis. The evolution of the in-plane lattice constant during the growth is deduced from the inter-reticular spacing between the (1 0) and the (−1 0) diffraction streaks. Figure 1 displays the increase in the lattice constant during

a)Electronic mail: ludovic.desplanque@iemn.univ-lille1.fr.

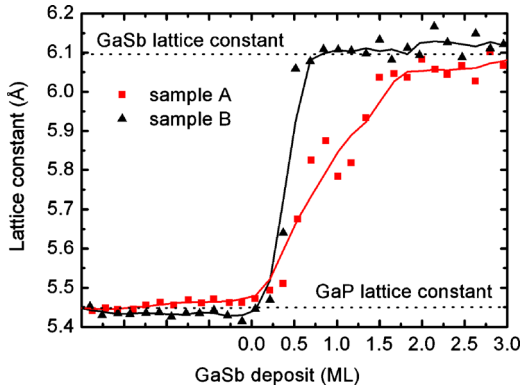

FIG. 1. (Color online) Lattice constant evolution during the first 3 GaSb ML deposition on a Ga-rich (sample A) and an Sb-rich (sample B) GaP surface.

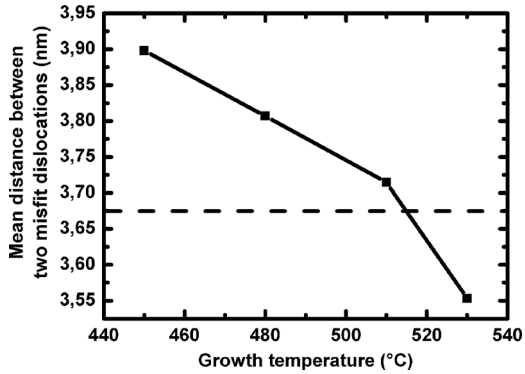

FIG. 3. Mean distance between MDs at the GaSb/GaP interface vs GaSb growth temperature. The ideal distance for a perfect relaxation by 90° MDs (S_{ideal}) is indicated by the horizontal dashed line.

the first 3 ML of the GaSb growth. For both samples, a quick change from the GaP lattice constant (5.4505 Å) to a value close to that of GaSb (6.095 Å) occurs during the first monolayer. However, this relaxation is faster for sample B (about 0.7 ML) than for sample A (about 1.6 ML) and the lattice constant after 3 ML is a bit larger for sample B than for sample A (about 6.1 Å versus 6.05 Å). This suggests a better relaxation for sample B than for sample A. After deposition of 10 GaSb ML, the AFM images (not shown) recorded on both samples reveal roughly the same surface morphology, i.e., an island density around $1.8\times10^{10}/\mathrm{cm}^2$ and a mean island height of 9 nm. Differences between samples A and B are highlighted by the cross-sectional high-resolution TEM images presented in Fig. 2. The interfaces between GaSb and GaP are underlined by MDs, as indicated by the white arrows which mark the termination of the additional {111} lattice planes in the GaP substrate. In these images recorded along the $[1\bar{1}0]$ zone axis, the core position of 60° and 90° MDs is marked by the termination of one and two additional {111} half lattice planes, respectively. Therefore, as can be seen in Fig. 2(a), sample A exhibits mainly 60° MDs because the

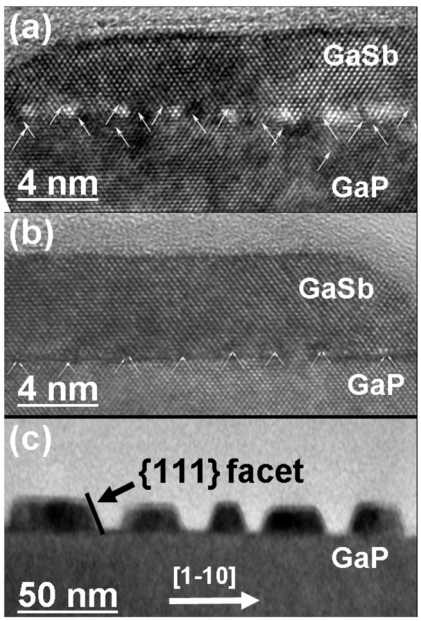

FIG. 2. Cross-sectional high-resolution TEM images along the $[1\bar{1}0]$ zone axis of the (a) samples A and [(b) and (c)] B. Arrows indicate 60° and 90° misfit dislocations at the interface between the substrate and buffer layer.

additional half lattice planes are all separated. The 60° MDs are distributed in a 3 nm wide interfacial zone extending on both sides of the nominal interface. In contrast, sample B shows a regular periodic array of 90° MDs confined at the interface. Eventually, the islands in the latter case are flatter. On Fig. 2(c), displaying a larger cross section of sample B, we can observe that the different GaSb islands of the sample exhibits {111} facets and the same height and flatness. From the results of Figs. 1 and 2, one can deduce that an Sb-rich GaP surface promotes the formation of a regular array of 90° MDs that are more efficient for GaSb relaxation.

The array of 90° MDs observed in Fig. 2(b) exhibits a period of about 3.80 nm. This mean value is statistically obtained after the TEM cross section observations on several islands. The same measurement is performed for different growth temperatures (samples C, D, and E) from 450 to 530 °C. The results are presented in Fig. 3. For a 100% relaxation of the GaSb overlayer, the theoretical distance between two 90° dislocations is given by $S=b/f=(a_f\cdot a_s)/[\sqrt{2}(a_f-a_s)]$, where b is the Burger's vector, f is the lattice mismatch between the layer and the substrate, and a_f and a_s are the layer and substrate lattice parameters, respectively. For the GaSb/GaP system, S amounts to 3.675 nm (dashed line in Fig. 3). This figure shows that high growth temperatures promote island relaxation (510 °C). At 530 °C, the measured distance between dislocations is smaller than the theoretical value: this is due to the formation of many 60° MDs. This result is consistent with the above results relative to the surface preparation. Indeed, the increase of the growth temperature favors Sb re-evaporation turning back to the case of a Ga-rich surface, where 60° MDs appear rather than 90° MDs.

The above observations are in agreement with those reported earlier during the growth of GaSb on (001) GaAs.[5,6,8] However, in our case, the mismatch is ~12% instead of ~8% for the GaSb/GaAs system. This tends to show that the growth of fully relaxed islands via 90° MDs is probably a common feature for highly mismatched material systems. A possible explanation for the formation of 90° MDs is the nucleation at the leading edge of advancing {111} planes of the islands and the gliding inward as proposed previously for the GaSb/GaAs case.[5,6] This mechanism seems to be promoted by starting the GaSb growth on a Sb-rich surface.[8]

After optimization of the surface preparation and growth temperature, a high mobility AlSb/InAs heterostructure is grown on a semi-insulating (001) GaP substrate (Fig. 4). Ac-

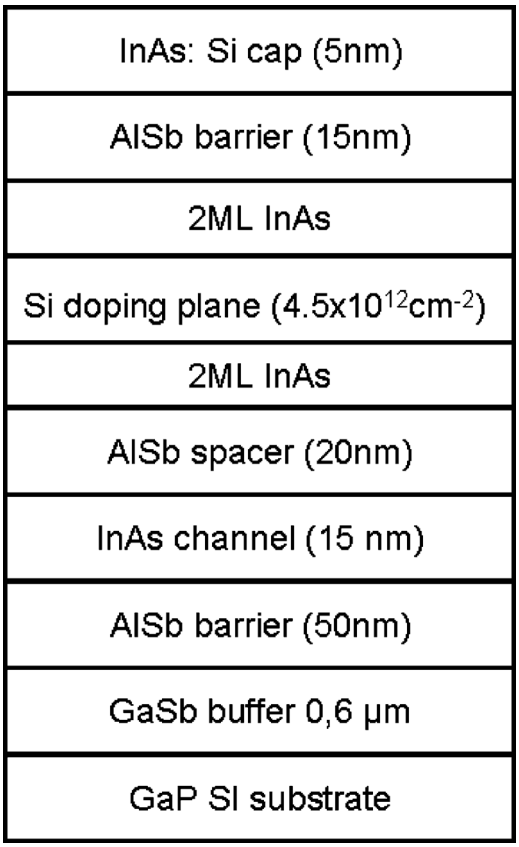

FIG. 4. Schematic of the AlSb/InAs high electron mobility heterostructure grown on GaP.

cording to the above results, we use an Sb-rich GaP surface preparation and a 600 nm GaSb buffer layer grown at 510 °C. Details about the heterostructure growth have already been reported.[4] The sample exhibits a 0.27 nm rms surface roughness measured by AFM on a 1×1 μm^2. RT and 77 K transport properties of the heterostructure are studied by Hall effect measurements using the Van der Pauw configuration. We attain mobilities of 25 500 $cm^2\ V^{-1}\ s^{-1}$ at 300 K and 108 000 $cm^2\ V^{-1}\ s^{-1}$ at 77 K with sheet carrier densities of 2×10^{12} and 1.6×10^{12} cm^{-2}, respectively. Even if these values are a bit lower than the best ones reported on GaAs or InP, they compare rather well with the one reported by Lin *et al.*[15] using a ten times thicker buffer layer for the same lattice mismatch.

Our results clearly show that an Sb-rich GaP surface preparation promotes the growth of flat and relaxed GaSb islands via the formation of a periodic array of 90° MDs at the GaSb/GaP interface. A complete relaxation is achieved by increasing the growth temperature while keeping Sb-rich growth conditions. Under these optimized conditions, a high electron mobility AlSb/InAs heterostructure is demonstrated exhibiting values of 25 500 $cm^2\ V^{-1}\ s^{-1}$ at RT and higher than 100 000 $cm^2\ V^{-1}\ s^{-1}$ at low temperature. This result is very promising for the integration of high speed and low power Sb-based electronic devices in the silicon technology.

This work is supported by the National Research Agency under project MOS35, Contract No. ANR-08-NANO-022.

[1]B. R. Bennett, R. Magno, J. B. Boos, W. Kruppa, and M. G. Ancona, Solid-State Electron. **49**, 1875 (2005).
[2]C. A. Chang, L. L. Chang, E. E. Mendez, M. S. Christie, and L. Esaki, J. Vac. Sci. Technol. B **2**, 214 (1984).
[3]G. Tuttle, H. Kroemer, and J. H. English, J. Appl. Phys. **65**, 5239 (1989).
[4]L. Desplanque, D. Vignaud, and X. Wallart, J. Cryst. Growth **301–302**, 194 (2007).
[5]A. Rocher and E. Snoeck, Mater. Sci. Eng., B **67**, 62 (1999).
[6]W. Qian, M. Skownroski, R. Kaspi, M. De Graef, and V. P. Dravid, J. Appl. Phys. **81**, 7268 (1997).
[7]S. H. Huang, G. Balakrishnan, A. Khoshakhlagh, A. Jallipalli, L. R. Dawson, and D. L. Huffaker, Appl. Phys. Lett. **88**, 131911 (2006).
[8]S. Huang, G. Balakrishnan, and D. L. Huffaker, J. Appl. Phys. **105**, 103104 (2009).
[9]A. Bourret and P. H. Fuoss, Appl. Phys. Lett. **61**, 1034 (1992).
[10]A. Vilà, A. Cornet, J. R. Morante, P. Ruterana, M. Loubradou, R. Bonnet, Y. Gonzales, and L. Gonzales, Philos. Mag. A **71**, 85 (1995).
[11]K. Akahane, N. Yamamoto, S. Gozu, and N. Ohtani, J. Cryst. Growth **264**, 21 (2004).
[12]Y. H. Kim, J. Y. Lee, Y. G. Noh, M. D. Kim, S. M. Cho, Y. J. Kwon, and J. E. Oh, Appl. Phys. Lett. **88**, 241907 (2006).
[13]S. H. Huang, G. Balakrishnan, A. Khoshakhlagh, L. R. Dawson, and D. L. Huffaker, Appl. Phys. Lett. **93**, 071102 (2008).
[14]I. Németh, B. Kunert, W. Stolz, and K. Volz, J. Cryst. Growth **310**, 1595 (2008).
[15]Y. C. Lin, H. Yamaguchi, E. Y. Chang, Y. C. Hsieh, M. Ueki, Y. Hirayama, and C. Y. Yang, Appl. Phys. Lett. **90**, 023509 (2007).